

# Lawrence Berkeley Laboratory

UNIVERSITY OF CALIFORNIA

## Materials & Molecular Research Division

Submitted to Metallurgical Transactions A

THE THERMOELASTIC PHASE TRANSITION IN Au-Cd ALLOYS  
STUDIED BY ACOUSTIC EMISSION

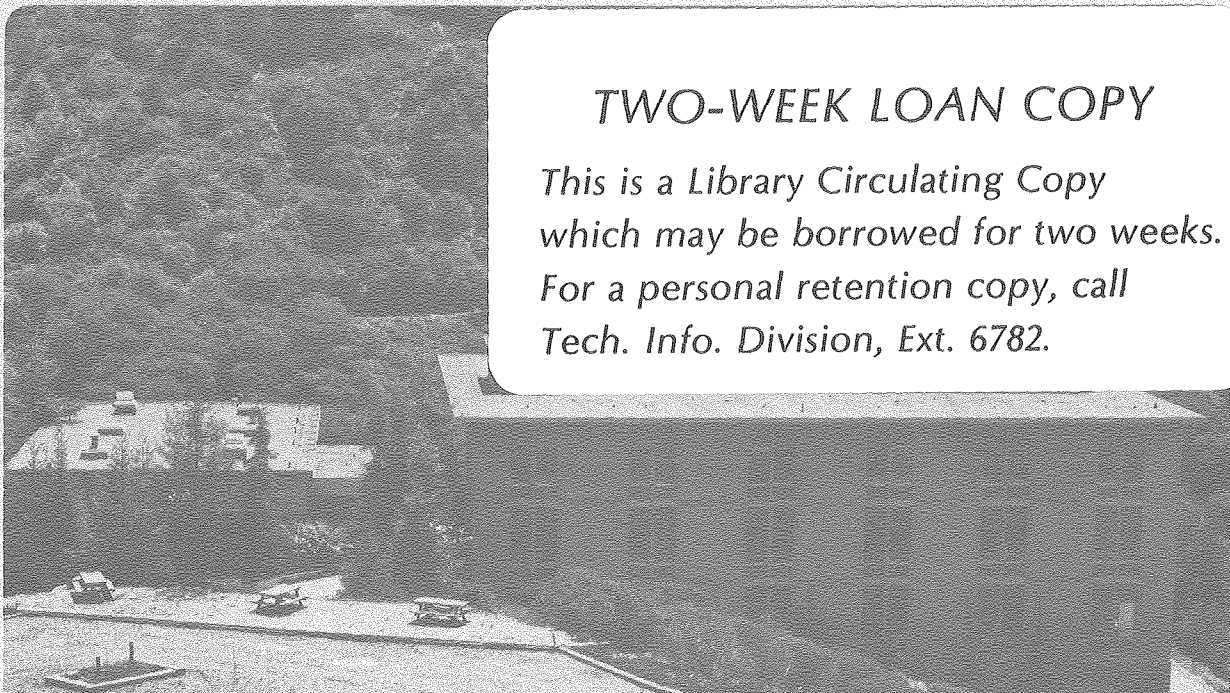
I. Baram and M. Rosen

March 1980

RECEIVED  
LAWRENCE  
BERKELEY LABORATORY

APR 18 1980

LIBRARY AND  
DOCUMENTS SECTION



### TWO-WEEK LOAN COPY

*This is a Library Circulating Copy  
which may be borrowed for two weeks.  
For a personal retention copy, call  
Tech. Info. Division, Ext. 6782.*

## **DISCLAIMER**

This document was prepared as an account of work sponsored by the United States Government. While this document is believed to contain correct information, neither the United States Government nor any agency thereof, nor the Regents of the University of California, nor any of their employees, makes any warranty, express or implied, or assumes any legal responsibility for the accuracy, completeness, or usefulness of any information, apparatus, product, or process disclosed, or represents that its use would not infringe privately owned rights. Reference herein to any specific commercial product, process, or service by its trade name, trademark, manufacturer, or otherwise, does not necessarily constitute or imply its endorsement, recommendation, or favoring by the United States Government or any agency thereof, or the Regents of the University of California. The views and opinions of authors expressed herein do not necessarily state or reflect those of the United States Government or any agency thereof or the Regents of the University of California.

THE THERMOELASTIC PHASE TRANSITION IN Au-Cd ALLOYS

STUDIED BY ACOUSTIC EMISSION

---

by

I. Baram

Materials Engineering Department

Ben Gurion University, Beer Sheva, Israel

and

M. Rosen\*

Molecular and Materials Research Division

Lawrence Berkeley Laboratory

University of California, Berkeley, USA

\*On leave from the Materials Engineering Department, Ben Gurion  
University, Beer Sheva, Israel.



ABSTRACT

The acoustic emission generated during the thermoelastic phase transitions in polycrystalline Au-47.5 at.% Cd and in Au-49 at.% Cd alloys was recorded and analyzed. The emission detected is a manifestation of the frictional energy dissipated by the moving interfaces during the nucleation and growth stages of the reversible phase transitions. It was found that the amount of energy dissipated depends upon the direction of the transformation, the heating or cooling rates, and the specific crystallographic features of the martensitic phases. Premartensitic acoustic activity was detected in both alloys at temperatures of about 25°C before the  $M_s$  point. The dynamics and kinetics of martensitic thermoelastic phase transformations are discussed in terms of the accompanying generation of acoustic emission.

## INTRODUCTION

Acoustic emission is a transient elastic wave generated by a rapid release of energy within the material.<sup>1</sup> It has been shown to be a useful technique in studying martensitic phase transformations.<sup>2-5</sup> Analysis of the occurrence and character of the acoustic emission signals yields an insight into the kinetics and dynamics of the elastic fields in the crystal lattice. In this context, of particular interest are the thermoelastic martensites, and especially those exhibiting a shape memory effect in which the reverse martensite-parent phase transformation is biased by the elastic energy stored during the forward martensitic transformation.<sup>6</sup> Changes in the local elastic fields occurring in the bulk are detected at the specimen surface, and subsequently analyzed by sensitive piezoelectric and electronic devices.<sup>7-10</sup> The objective of the present study was to determine the characteristic features of the thermoelastic phase transformations in Au-47.5 at.% Cd and Au-49.0 at.% Cd as manifested by the generation of acoustic emission signals.

## EXPERIMENTAL

Polycrystals of Au-47.5 at.% Cd and Au-49.0 at.% Cd were heated and cooled through their respective phase transformation ranges, between 10 and 120°C and back, at controlled heating and cooling rates. A copper-constantan thermocouple was attached to the specimens by means of an organic adhesive. The accuracy in the temperature measurements was  $\pm 0.5^\circ\text{C}$ . A stainless steel rod was used as an acoustic waveguide being coupled to a PZT transducer of a resonant frequency in the 150-300 kHz range. The overall amplification of the electronic detection system was set to 80 dB. Filtered signals exceeding the threshold peak amplitude value of 1V

after amplification, were recorded simultaneously as cumulative counts (threshold crossings), cumulative events and count rate as a function of temperature. At the end of each cooling/heating cycle, the distribution of the acoustic emission events, according to their peak amplitude, was obtained by means of a distribution analyzer module.

A schematic of the heating/cooling device is given in Fig. 1. The block diagram of the data acquisition system is given in Fig. 2.

## RESULTS

Both alloys were heated and cooled at a rate of  $1^{\circ}\text{C}/\text{min}$ . In a separate set of experiments, both alloys were heated and cooled consecutively four times at a rate of  $3^{\circ}\text{C}/\text{min}$ . The numerical results of the cumulative counts and events, presented in Tables 1 and 2, were normalized to a unit molar volume. The  $M_s$  and  $A_s$  temperatures are shown in these tables, as well as the temperatures at which the last acoustic activity was recorded. "Pre-martensitic" and "preaustenitic" pulses were detected at temperatures significantly before the  $M_s$  and  $A_s$  temperatures in specimens that underwent several heating/cooling cycles. This behavior was absent in specimens cycled only once and in specimens in which the rest period between consecutive cycles exceeded 24 hours at room temperature.

Typical acoustic emission behavior is shown in Figs. 3-6. Each figure shows the evolution of the cumulative number of acoustic counts, as well as the count-rate as a function of temperature. The  $M_s$  and  $A_s$  temperatures, as tabulated in Tables 1 and 2, are the temperatures at which the count rates change drastically. The transformation temperatures appear to be sensitive to the cooling and heating rates. The acoustic activity, evaluated as the total number of counts during the whole transformation

range, depends upon the direction of the transformation (heating or cooling) as well as upon the rates of temperature change. The comparative acoustic activity is shown in Table 3, where the activity of the Au-47.5 at.% Cd alloy on heating is taken as unity. The acoustic activity during the transformation from the high temperature phase (htp) to the low temperature phase (ltp) is significantly smaller, for both cooling rates, than at the reverse transformation. It is about 10 times smaller for Au-47.5 at.% Cd alloy, and about 100 times smaller for the 49.0 at.% Cd alloy.

The average number of counts per acoustic event is an acoustic emission parameter that reflects the peak amplitude of the event and is, therefore, a measure of the dissipated elastic energy.<sup>11</sup> The htp  $\rightarrow$  ltp and the reverse transformations yielded different values for this acoustic emission parameter, being about 5 times larger during the transformation on heating than on cooling.

The envelope of the count rate curves, during both heating and cooling stages, is generally bell-shaped (Figs. 3-6), passing through a maximum value followed by a gradual decrease. This reflects the fact that the acoustic activity curves (cumulative counts) are S-shaped, thus exhibiting the thermoelastic nature of the transformation, in both directions. A similar behavior was observed in Ti-Al and Ni-Al alloys.<sup>10</sup> Acoustic emission did invariably stop, whenever heating (or cooling) was stopped. Resumption of the temperature variation process caused further generation of acoustic emission. From the envelope of the count rate curves one can estimate the approximate width of the transformation range. The following values were found for both alloys: 12 and 4.5°C at heating rates of 3 and 1°C/min, respectively, and 8 and 3°C at cooling rates of 3 and 1°C/min, respectively.

The bell-shaped feature is less distinct for the htp  $\rightarrow$  ltp transformation in the Au-49.0 at.% Cd alloy.

A phase stabilization phenomenon was observed when specimens of Au-47.5 at.% Cd and Au-49.0 at.% Cd were heated only up to 90 and 70°C, respectively. No acoustic activity whatsoever was detected during the subsequent cooling sequence.

## DISCUSSION

In acoustic emission studies various parameters have been used to characterize the emission yield such as the ringdown count, count rate, and r.m.s. voltage. Emission pulses can be considered as acoustic events and their amplitude analyzed. In the ringdown mode it is assumed that the number of counts, i.e., the number of crossings of a fixed threshold, obtained during a deformation test, is related to the peak amplitude of the acoustic event through a damped sinusoidal relationship.<sup>11</sup> However, when the dependence of the ringdown counting on signal peak amplitude and trigger level was examined in acoustic emission during a martensitic transformation, the relationship was found to be linear rather than logarithmic.<sup>12</sup> In this case, the number of counts produced by an event of peak amplitude  $V_i$  is:

$$N(V_i) = a(V_T)V_i + C(V_T) \quad (1)$$

where  $V_T$  is the threshold trigger level. When amplitude distribution analysis is applied, the peak voltage of the emission burst is the acoustic emission parameter. The number of detected events  $n(V_i)$ , with peak amplitudes larger than  $V_i$  may be fitted to an equation of the following form<sup>13</sup>:

$$n(V_i) = P \left( \frac{V_T}{V_i} \right)^f \quad (2)$$

where  $P$  is the total number of events having peak amplitudes exceeding  $V_T$ .

The number of events having peak amplitudes between  $V_i$  and  $V_i + dV_i$  is:

$$m(V_i) = \frac{dn(V_i)}{dV_i} = \frac{Pb}{V_i} \left( \frac{V_T}{V_i} \right)^b \quad (3)$$

The number of ringdown counts produced by  $m(V_i)$  events having peak amplitudes  $V_i$  is  $m(V_i) \cdot N(V_i)$ .

The total number of counts produced during a whole experiment is:

$$N(\infty) = \int_{V_T}^{V_\infty} m(V_i) \cdot N(V_i) dV_i = P \left[ \frac{a \cdot b \cdot V_T}{b-1} + C \right] \quad (4)$$

Taking  $V_T = 1$  Volt,  $a = 3$  and  $C = -2$  <sup>(12)</sup>

$$N_\infty = P \frac{b+2}{b-1} = P \cdot \alpha \quad (5)$$

where  $\alpha$  is the average number of counts per event. Parameter  $\alpha$  is obtained directly from the experimental data, and is related to the sum of the acoustic amplitudes processed by the piezoelectric transducer, i.e., to the total voltage output from the signal processing system:

$$V(\text{total}) = \int_{V_T}^{V_\infty} m(V_i) V_i dV_i = P \frac{b}{b-1} = P \frac{(2+\alpha)}{3} \quad (6)$$

where  $P$  is the total number of events recorded during the course of the experiment.

The equivalent acoustic pressure  $P_o$  at the transducer - specimen interface is:

$$P_o = \frac{V(\text{total})}{G \cdot g} \quad (7)$$

where  $g$  is the transducer sensitivity and  $G$  is the gain of the electronic system. The total acoustic energy (in joules) is then:

$$W = 10^{-7} \frac{P_o^2 S}{\rho v} \quad (8)$$

where  $S$  is the surface of the transducer,  $\rho$  is the density of the specimen, and  $v$  is the sound velocity, in cgs units.

The acoustic portion of the dissipated energy during the phase transformation may be evaluated from the experimentally acquired acoustic emission parameters:

$$W(\text{joules}) = P^2 \frac{(\alpha+2)^2}{3} \frac{10^{-7}}{G^2 \cdot g^2} \cdot \frac{S}{\rho v} \quad (9)$$

The treatment presented here neglects the consideration of the following two points. Firstly, the acoustic energy reaching the specimen-transducer interface is only a part of the dissipative acoustic energy generated in the bulk. When the acoustic waves propagate through the specimen and waveguide they undergo a reduction in amplitude due to wavefront expansion and ultrasonic wave attenuation. Secondly, the frequency dependence of the detected voltage amplitudes has not been considered. The relatively narrow frequency ranges of the piezoelectric transducer and the frequency

limitations of the measurement system do not permit the processing of the full frequency content of the source signal, as generated in the bulk. Nevertheless, it is plausible to assume a linear relationship between the released and recorded acoustic energy. The acoustic emission parameter  $\alpha$ , which is the average number of counts per event, recorded during the experiment, is related through Eq. 9 with the acoustic portion of the dissipated energy. Moreover, an estimate can be made of the acoustic energy reaching the transducer during the course of the phase transformation. The numerical values of this energy are given in Table 4. Noteworthy is the dependence of the heating/cooling rate on the magnitude of the acoustic energy, the drastic changes for thermal direction of the thermoelastic transformation, and the difference in the energy values for the alloys investigated.

Formation of a martensite plate causes a macroscopic change of shape. Although the invariant plane strain minimizes the strain along the habit plane, an effective strain can be developed as the martensite plate grows in a third dimension. In polycrystals, in the absence of external stresses, and where differently oriented martensite plate variants form, the growth of each plate may be impeded by grain boundaries or by adjacent plates. At the tapered ends of the plates the invariant plane strain condition is no longer fulfilled, and dislocations will be present at the ends of the tapers.<sup>15</sup> Local elastic fields in the lattice will change in a sufficiently abrupt manner during the martensitic plate growth, thus generating detectable acoustic emission. The dissipated energy is the elastic strain energy due to the frictional resistance opposing the interfacial motion during the martensitic phase transformation. The frictional resistance has been shown<sup>16</sup> to contribute to the observed thermodynamic changes during

the phase transformation in Cu-14Al-2.5Ni alloy. The net enthalpy changes during the parent phase to martensite transformation are reduced when the transformation occurs in a polycrystal. Olson and Cohen<sup>17</sup> have shown:

$$\Delta G_{ch}^{A \rightarrow M} + \eta G_{el} + V_m \tau_o \gamma_T = 0, \text{ on cooling} \quad (10)$$

$$\Delta G_{ch}^{M \rightarrow A} + \eta G_{el} - V_m \tau_o \gamma_T = 0; \text{ on heating} \quad (11)$$

where  $\Delta G_{ch}$  and  $\Delta G_{el}$  are the chemical and elastic free energy changes per mole, respectively,  $V_m$  is the molar volume and  $\tau_o$  is the shear stress required to move an interface thus yielding the transformational shear strain  $\gamma_T$ . An additional term should be added which takes into account the stress needed to overcome obstacles to the interface movement, such as grain boundaries, existing interfaces and defects.

Equations 10 and 11 indicate that the frictional energy dissipated during the transformation,  $W_f = V_m \tau_o \gamma_T$ , decreases on cooling when  $\Delta G_{el}$  increases, and the reverse on heating. The acoustic emission energy, recorded by the piezoelectric transducer, arises from the dissipation phenomenon in the bulk. It is not known to what extent the frictional work transformed into acoustic emission energy. However, the qualitative significance of the experimental results can be established. In polycrystalline multiple-interface martensitic transformation, the acoustic activity will be appreciably higher in the reverse transformation (ltp  $\rightarrow$  htp) than in the direct one. This behavior is shown in Tables 3 and 4.

The magnitude of the acoustic energy detected during the martensitic phase transformation in Au-49.0 at.% Cd alloy is by two orders of magnitude lower than in the 47.5 at.% Cd alloy. The difference may be due to the different crystallographic features of the martensites in these two alloys.

The parent phases in both alloys have a CsCl(B2) structure of a space group  $Pm\bar{3}m$ . The Au 47.5 at.% Cd alloy transforms into an orthorhombic (B19) twinned martensite of space group  $Pmmm$ . There are 24 possible crystallographic variants for this structure. All of them are probably activated during the phase transformation. The Au-49.0 at.% Cd alloy transforms into an hexagonal trigonal twinned structure ( $P\bar{3}m1$ ) with a larger number of crystallographic variants when a multiple interface transformation occurs, namely 36 for the trigonal structure. During the course of the martensitic transformation more elastic energy is stored in the trigonal phase than in the orthorhombic one. The chemical free energy change is, of course, different for each alloy. As an overall effect, it appears that the dissipated elastic energy is smaller in the trigonal than in the orthorhombic structure. Neither cycling nor cooling rate affects the amount of dissipated energy in the 49.0 at.% Cd alloy. The increased amount of dissipated energy, observed in Au-47.5 at.% Cd alloy, when cooling rate is increased, may be interpreted as due to an enhancement of the barrier density opposing the movement of transformation interfaces in the orthorhombic structure.

The lower the energy dissipated during the direct martensitic transformation ( $htp \rightarrow ltp$ ), the higher was the acoustic energy detected during the reverse transformation. This experimental observation is in agreement with Eqs. 10 and 11. Thermal cycling lowers the  $A_s$  temperature (Tables 1 and 2) for both alloys, as a result of the thermodynamic balance where the dissipated elastic energy is only one contributing factor. The fact that the acoustic energy detected during the  $ltp \rightarrow htp$  transformation in Au-49.0 at.% Cd alloy is higher than the energy in the Au-47.5 at.% Cd is consistent with the proposed dissipation mechanism.

Mention should be made of the so-called "premartensitic" and "preaustenitic" pulses in the acoustic emission. Soft lattice vibration modes have been observed, and diffuse X-ray diffraction effects have been detected at temperatures above the  $M_s$  in several thermoelastic alloys.<sup>18</sup>

There is some controversy as to the interpretation of these phenomena, either as a gradual elastic softening of the lattice approaching the transformation temperature, or a manifestation of higher order phase transitions when atomic shuffling occurs before the "critical" temperature is attained. In the present investigation, a definite "premartensitic" acoustic activity was detected at about 25°C before the  $M_s$  temperature in both the Au-Cd alloys. This activity could not be detected when a single heating/cooling cycle was performed, neither at the first of a series of successive thermal cycles, nor when more than 24 hours elapsed between one cycle and another. In general, the "premartensitic" activity in thermally cycled specimens is rather low, appearing as 2-3 discrete pulses at low rates. This phenomenon needs further elucidation particularly emphasizing the effect of rest times on the relaxation of stresses and phase stabilization induced by the phase transformation.

## CONCLUSIONS

1. During the martensitic transformations in polycrystalline Au-47.5 and Au-49.0 at.% Cd alloys, a part of the elastic strain energy due to the frictional resistance opposing interfacial motion is dissipated and recorded as acoustic emission.
2. When a particular acoustic emission parameter is used, namely the average number of counts per acoustic event, an estimate can be made of the amount of energy dissipated during the phase transitions.

3. The acoustic energy detected during the phase transformations depends on the direction of the thermal cycle, on the heating or cooling rates, and on the specific crystallographic features of the martensitic phase.
4. The acoustic energy detected during the htp  $\rightarrow$  ltp (parent phase to martensite transition) is by 2-3 orders of magnitude lower than the energy detected during the reverse transformation.
5. "Premartensitic" acoustic activity was observed in both alloys at temperatures of about 25°C before the Ms temperatures.

#### ACKNOWLEDGMENTS

The able technical assistance of A. Cohen in performing the acoustic emission experiments and the fruitful discussions with Y. Gefen are greatly appreciated. This work was performed in the AE laboratory of the Materials Engineering Department, Ben Gurion University, Beer Sheva, Israel with the support by a grant from the Israeli National Council for Research and Development.

This work was supported by the U.S. Department of Energy under Contract W-7405-ENG-48.

# REFERENCES

1. Acoustic Emission Working Group in Acoustic Emission, S.T.P. 505, Baltimore, ASTM, 1972, 335-337.
2. R. G. Liptai, H. L. Dunegan and C. A. Tatro, Int. J. Nondestructive Testing, 1978, Vol. 1, p. 213.
3. G. R. Speich and R. M. Fisher, Acoustic Emission, S.T.P. 505, Baltimore, ASTM, 1972, pp. 140-151.
4. K. Ono, T. C. Schlotthauer and T. J. Koppenaal, UCLA-ENG-7334 Report, May 1973.
5. G. R. Speich and A. J. Schwoeble, Monitoring Structural Integrity by Acoustic Emission, S.T.P. 571, Philadelphia, ASTM, 1975, p. 10-58.
6. C. M. Wayman in Shape-Memory Effects in Alloys, edited by J. Perkins, Plenum Press, New York, 1975, pp. 128.
7. R. I. Mints, V. P. Meleklín, I. Yu. Ievlev and V. V. Bukhaleukov, Soviet Phys.--Solid State, 1972, Vol. 14, p. 1368.
8. I. Yu. Ievlev, V. P. Meleklín, R. I. Mints, and V. M. Segal, Soviet Phys.--Solid State, 1974, Vol. 15, p. 1761.
9. R. Pascual, M. Ahleró, R. Rapacioli, and W. Arnesdo, Scripta Met., 1975, Vol. 9, p. 79.
10. J. Baram and M. Rosen, Scripta Met., 1979, Vol. 13, p. 565.
11. D. O. Harris and R. L. Bell, Experim. Mech., 1977, Vol. 17, p. 347.
12. E. Esmail and I. Grabec, Ultrasonics, 1978, Vol. 16, p. 87.
13. A. A. Pollock, in "Acoustic and Vibration Progress, ed. R. W. B. Stephens, H. G. Leventhall, Chapman and Hall, London, 1973, pp. 150.
14. H. M. Ledbetter and C. M. Wayman, Met. Trans. A., 1972, Vol. 3, p. 2349.

15. L. Delaey, R. V. Krischman, H. Tas and H. Warlimont, J. Mater. Sci., 1974, Vol. 9, p. 1521.
16. R. J. Salzbrenner and M. Cohen, Acta. Met., 1979, Vol 27, p. 739.
17. G. B. Olson and M. Cohen, "Thermoelastic Behavior in Martensitic Transformations," Scripta Met., Vol. 9, 1975, pp. 1247-1254.
18. Shape Memory Effects in Alloys, edited by J. Perkins, Plenum Press, New York, 1975.

CAPTION TO FIGURES

Figure 1. Heating/cooling device.

Figure 2. Data-acquisition system. Block diagram.

Figure 3. Au-47.5 at.% Cd - Heating.

Cumulative counts and count-rate vs. temperature.

Figure 4. Au-47.5 at.% Cd - Cooling

Cumulative counts and count-rate vs. temperature.

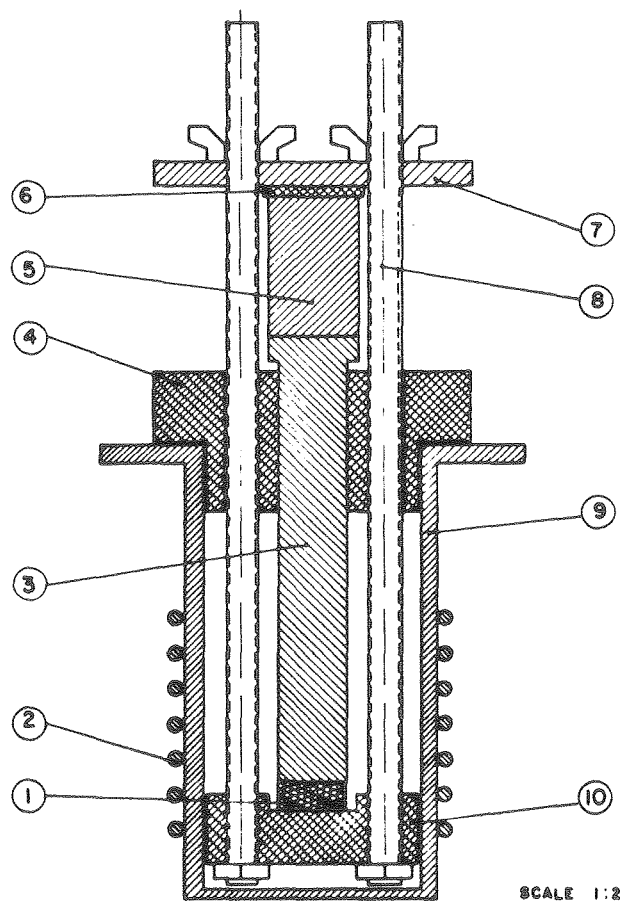
Figure 5. Au-49.0 at.% Cd - Heating

Cumulative counts and count-rate vs. temperature.

Figure 6. Au-49.0 at.% Cd - Cooling

Cumulative counts and count-rate vs. temperature.

## HEATING/COOLING DEVICE



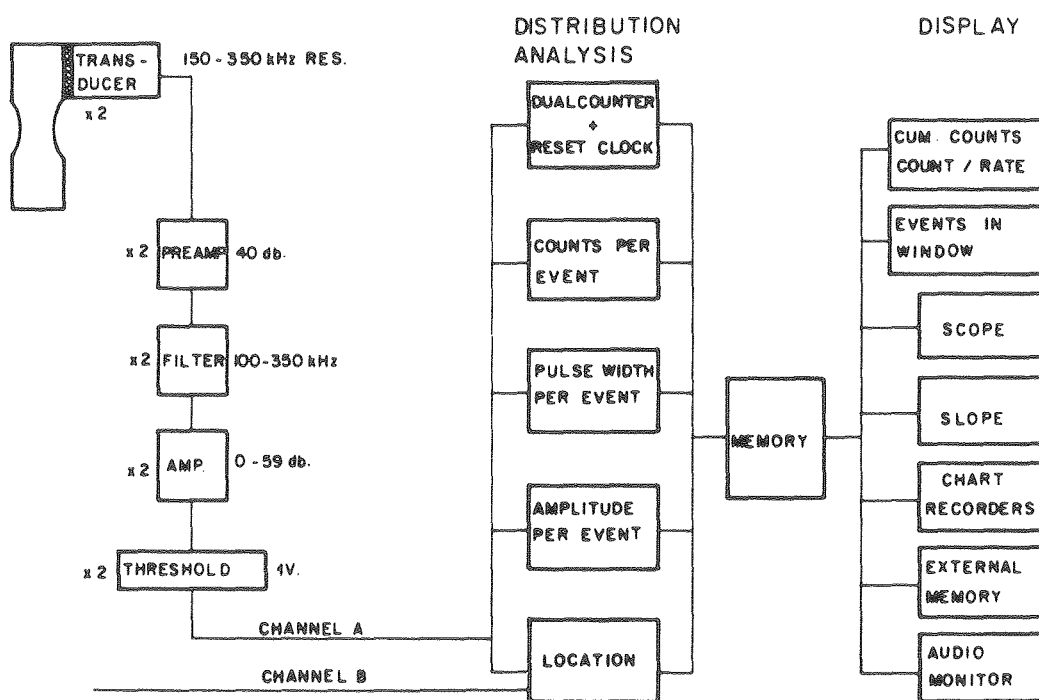
- |                         |                 |
|-------------------------|-----------------|
| ① SPECIMEN              | ⑧ TEFLON DISK   |
| ② HEATING COIL          | ⑦ METALLIC DISK |
| ③ WAVE GUIDE, STAINLESS | ⑥ GUIDING RODS  |
| ④ TEFLON SLEEVE         | ⑤ COPPER CAN    |
| ⑤ TRANSDUCER            | ⑩ TEFLON BASIS  |

THE COPPER CAN IS ABOVE LIQUID NITROGEN

XBL 803-8877

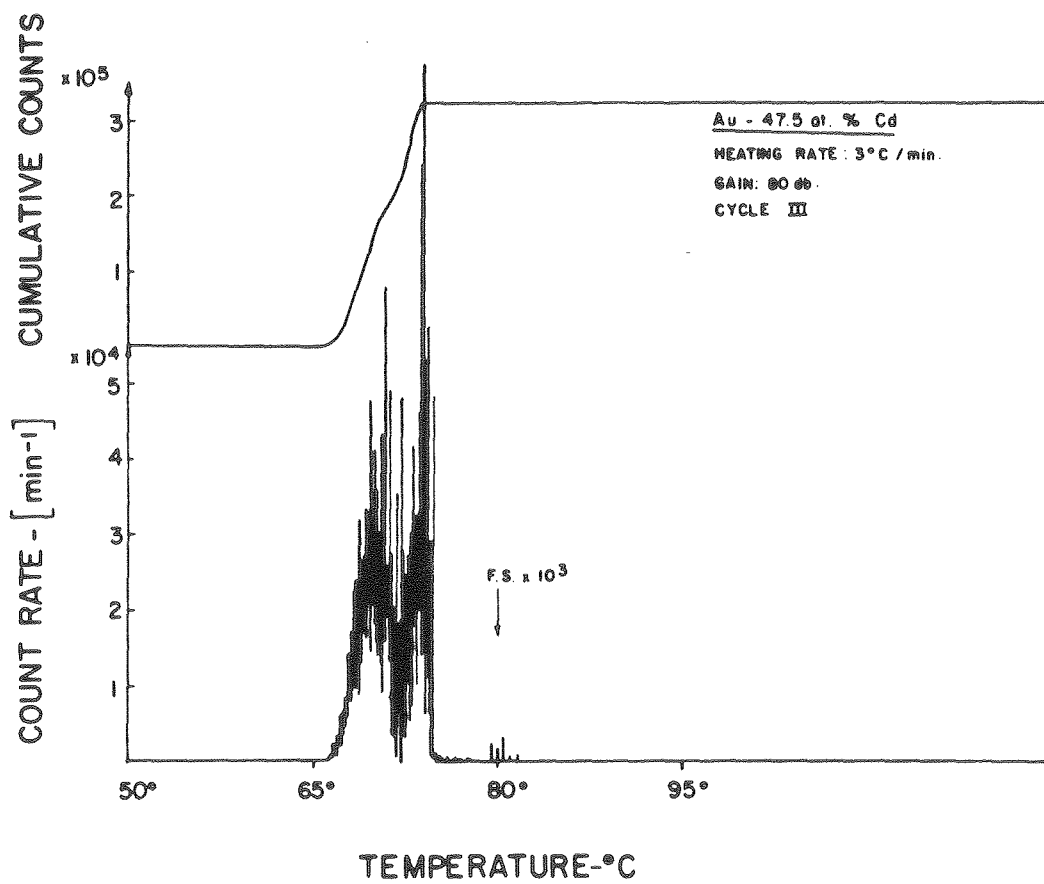
Fig. 1

# ACOUSTIC EMISSION DATA ACQUISITION SYSTEM BLOCK DIAGRAM



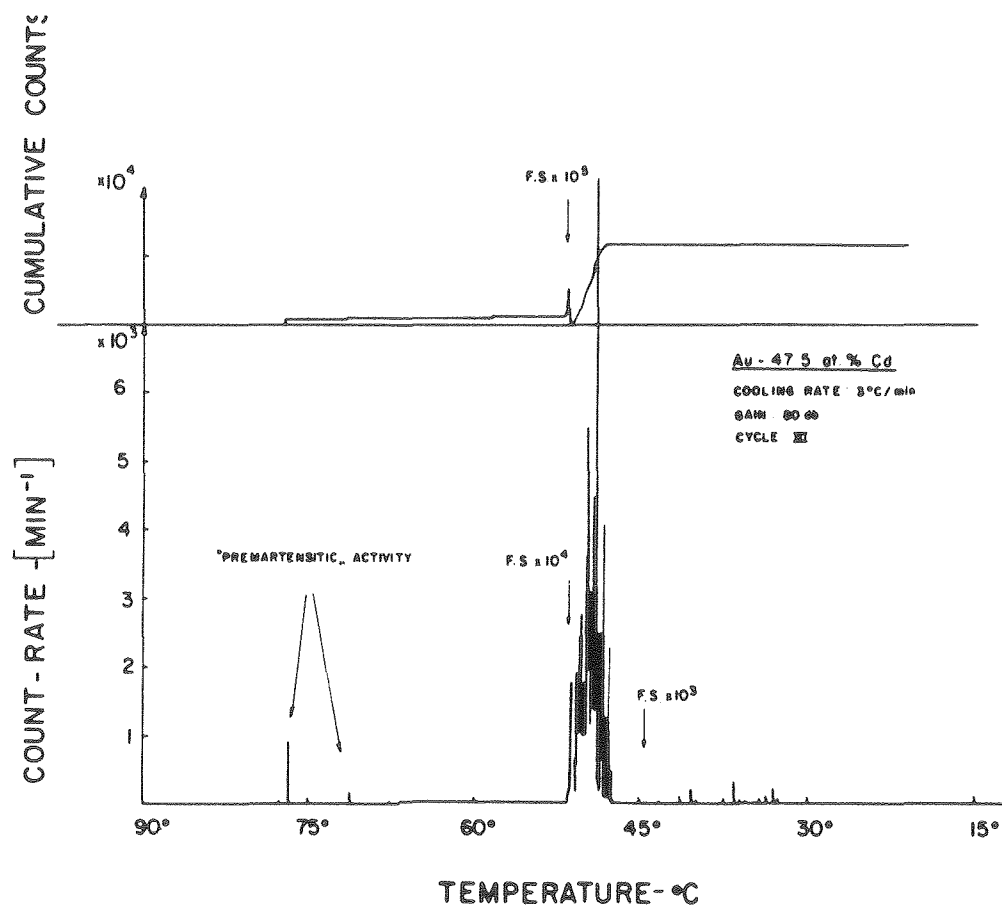
XBL 803-8876

Fig. 2



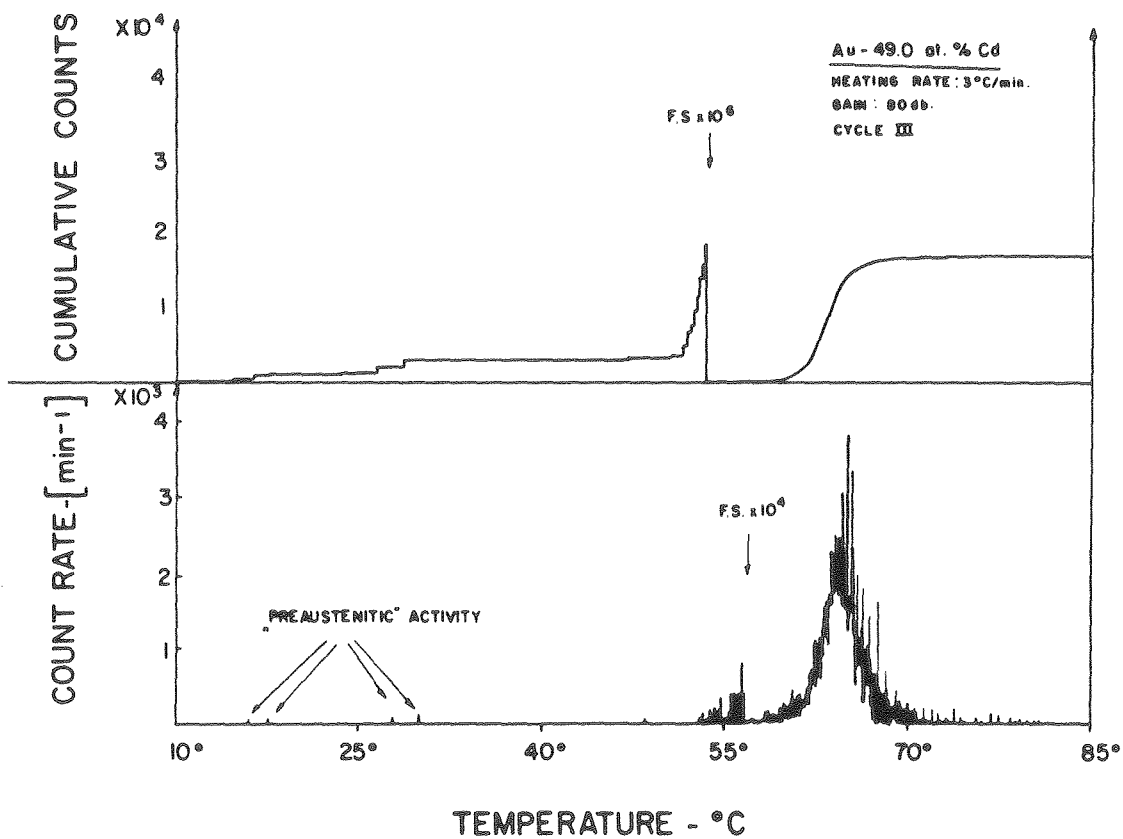
XBL 803-8875

Fig. 3



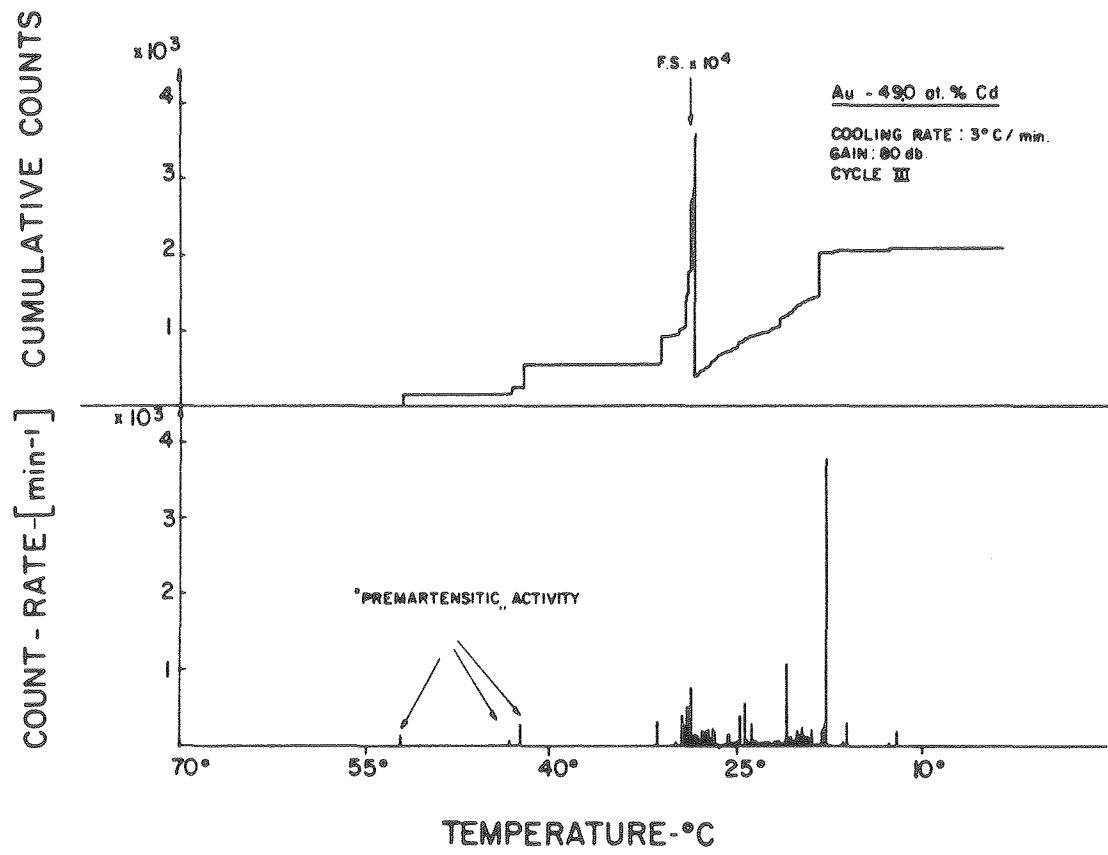
XBL 803-8874

Fig. 4



XBL 803-8873

Fig. 5



XBL 803-8856

Fig. 6

Table 1. Numerical Results - Au-47.5 at.% Cd

Cycle	1	1	2	3	4
Heating/Cooling Rate:	1°C/min	3°C/min	3°C/min	3°C/min	3°C/min
HEATING $A_g$	67.5°C	68°C	66.5°C	66°C	66°C
Premartensitic pulses	None	None	None	None	None
Last activity recorded	98°C	84°C	84°C	82°C	83°C
Cumulative counts, $N(=)$	$2.07 \times 10^7$	$2.24 \times 10^7$	$1.54 \times 10^7$	$1.53 \times 10^7$	$1.52 \times 10^7$
Cumulative events, P	$4.48 \times 10^5$	$4.62 \times 10^5$	$2.78 \times 10^5$	$2.74 \times 10^5$	$2.74 \times 10^5$
Average counts/event, $\alpha$	46	48	55	56	56
COOLING $M_g$	55°C	52.5°C	52.5°C	52°C	52°C
Premartensitic pulses	None	None	76°C	77°C	77°C
Last activity recorded	29°C	30°C	30°C	30°C	30°C
Cumulative counts, $N(=)$	$1.90 \times 10^6$	$5.28 \times 10^6$	$5.09 \times 10^6$	$5.66 \times 10^6$	$5.28 \times 10^6$
Cumulative events, P	$2.88 \times 10^5$	$5.94 \times 10^5$	$5.75 \times 10^5$	$5.38 \times 10^5$	$4.72 \times 10^5$
Average counts/events, $\alpha$	6.6	8.9	8.9	10.5	11.2

Table 2. Numerical Results - Au-49.0 at.% Cd

Cycle	I	I	II	III	IV
Heating/Cooling Rate:	1°C/min	3°C/min	3°C/min	3°C/min	3°C/min
HEATING $A_s$	58°C	56.5°C	53°C	53°C	53°C
Premartensitic pulses	None	None	13°C	15°C	Not available
Last activity recorded	88°C	87°C	88°C	85°C	87°C
Cumulative counts, $N(\infty)$	$4.86 \times 10^7$	$3.90 \times 10^7$	$2.92 \times 10^7$	$3.02 \times 10^7$	$3.16 \times 10^7$
Cumulative events, $P$	$1.38 \times 10^6$	$1.15 \times 10^6$	$1.00 \times 10^6$	$1.08 \times 10^6$	$1.12 \times 10^6$
Average counts/event, $\alpha$	35	34	29	28	28
COOLING $M_s$	28.5°C	29°C	28.5°C	29°C	29°C
Premartensitic pulses	None	None	49°C	52°C	51°C
Last activity recorded	6°C	9°C	9°C	10°C	10°C
Cumulative counts, $N(\infty)$	$5.77 \times 10^5$	$4.37 \times 10^5$	$4.54 \times 10^5$	$4.37 \times 10^5$	$4.54 \times 10^5$
Cumulative events, $P$	$1.10 \times 10^5$	$0.56 \times 10^5$	$0.56 \times 10^5$	$0.57 \times 10^5$	$0.57 \times 10^5$
Average counts/event, $\alpha$	5.2	7.8	8.1	7.6	7.9

Table 3. Comparative Acoustic Activities

Heating/cooling rate	<u>Au-47.5 at.% Cd</u>		<u>Au-49.0 at.% Cd</u>	
	1°C/min	3°C/min	1°C/min	3°C/min
Heating (first cycle)	1.0	1.1	2.3	1.9
Cooling (first cycle)	0.09	0.25	0.03	0.02

Table 4. Acoustic Energy Detected During the Phase-Transformation [ $\text{J}\cdot\text{mole}^{-1}$ ]

Cycle	Au-47.5 at.% Cd					Au-49.0 at.% Cd				
	1	1	2	3	4	1	1	2	3	4
Heating/Cooling Rate	<u>1°C/min</u>		<u>3°C/min</u>			<u>1°C/min</u>		<u>3°C/min</u>		
LTP → HTP Transformation	3.7	4.3	2.0	2.0	2.0	20.8	13.7	7.7	8.4	9.0
HTP → LTP Transformation	$4.9 \times 10^{-2}$	$3.4 \times 10^{-1}$	$3.1 \times 10^{-1}$	$3.6 \times 10^{-1}$	$3.1 \times 10^{-1}$	$5 \times 10^{-3}$	$2.4 \times 10^{-3}$	$2.6 \times 10^{-3}$	$2.4 \times 10^{-3}$	$2.6 \times 10^{-3}$

